Silicon–glass-based single piezoresistive pressure sensors for harsh environment applications

2013 J. Micromech. Microeng. 23 075020

(http://iopscience.iop.org/0960-1317/23/7/075020)

J. Micromech. Microeng. **23** (2013) 075020 (8pp) doi:10.1088/0960-1317/23/7/075020

Silicon–glass-based single piezoresistive pressure sensors for harsh environment applications

Haisheng San[1,2,5], Hong Zhang[1,2], Qiang Zhang[2], Yuxi Yu[3] and Xuyuan Chen[4,5]

[1] School of Physical and Mechanical and Electrical Engineering, Xiamen University, Xiamen 361005, People's Republic of China
[2] Pen-Tung Sah Institute of Micro-Nano Science and Technology, Xiamen University, Xiamen 361005, People's Republic of China
[3] Department of Materials Science and Engineering, College of Materials, Xiamen University, Xiamen 361005, People's Republic of China
[4] Department of Micro and Nano Systems Technology, Vestfold University College, PO Box 2243, N-3103 Tønsberg, Norway

E-mail: sanhs@xmu.edu.cn and xuyuan.chen@hive.no

Received 4 February 2013, in final form 11 May 2013
Published 11 June 2013
Online at stacks.iop.org/JMM/23/075020

Abstract
Silicon–glass (Si–glass)-based single piezoresistive pressure sensors were designed and fabricated by standard MEMS technology. The single piezoresistive sensing element was designed to be on the lower surface of the silicon diaphragm and be vacuum-sealed in a Si–glass cavity, which form a self-packaging protection structure helpful to the applications of sensors in harsh media. The pressure sensors were fabricated using a Si–glass anodic bonding technique, and the embedded Al feedthrough lines at the Si–glass interface are used to realize the electrical connections between the piezo-sensing element and the electrode-pads, and two larger-size electrode-pads are fabricated for realizing the soldered electrical connection between the sensor and the external circuit. The performance of the pressure sensors was characterized by a pressure test system at different temperature conditions. The temperature compensation was performed by the difference between the output voltage at zero-pressure and the output at operation pressure. The measurement results show that the sensitivity is 24 mV V^{-1} MPa^{-1}, the coefficient of sensitivity is 0.14% FS $^{\circ}C^{-1}$, and both the zero-point offset and the temperature coefficient of offset are equal to zero, which are able to meet the commercial application requirements. However, a nonlinearity of 5.2% FS caused by the balloon effect would considerably worsen the accuracy of the pressure sensor. It is suggested to reduce the balloon effect by using a bossed-diaphragm structure in the pressure sensor.

(Some figures may appear in colour only in the online journal)

1. Introduction

MEMS devices have made significant progress during the past two decades and many prototype devices have been demonstrated for a number of different applications. Many devices have been successfully commercialized, for example pressure sensors for automotive, industrial processing and biomedical applications [1–3]. At present, silicon piezoresistive pressure sensors are a mature technology in the industry, but when the pressure sensors are operated in harsh environments, such as high temperature, violent vibration and shock, high humidity, corrosive alkalis and acidity, and charged particles, their requirements in terms of reliability and stability are more rigorous than that of many advanced applications

[5] Authors to whom any correspondence should be addressed.

[4–7]. In order to protect the pressure sensors from harsh media while providing sensing access to the environment the device is supposed to interact with, much effort has been made on developing the proper protection methods for MEMS pressure sensors. Three general approaches have been taken. The first depends on using a coating material that protects the regions that need protection while providing access to those that need to interact with the external environment. For example, a passivation layer of oxide, nitride or carbide is deposited on the diaphragm surface of the pressure sensors to prevent direct exposure of the sensing elements to harsh media [8–10]. The second relies on using a liquid transmitting pressure technique to improve the pressure sensor packaging [9–11]. In this technique, the sensor chip is packaged in a cavity filled with silicon oil or silicone gel to keep it away from the external environment. The external pressure is transmitted to the chip through the oil or gel. The third depends on the package in the form of a shell or capsule that can be bonded to the device substrate to form a protective chamber [12, 13]. The main drawback of the first and second approaches is that the fragile sensor chips are likely to suffer contamination and damage during the wafer cleaning, dicing, assembling and wire bonding processes [14]. The third approach is known as wafer-level packaging, capable of providing wafer-level protection in package handling, but wafer-level packaging is always complicated and expensive, a quality which may potentially arise from the fabrication of the cap wafer and special packaging processes, such as reliable cap bonding and dice singulating. Therefore, if MEMS devices can participate in their own packaging (self-packaging), the packaging processes can be greatly simplified. In addition, the wire bonding technique is usually used in the electrical connection between MEMS chips and the external circuit, but it is not reliable for some applications in high-vibration environments. For example, in a tire pressure monitoring system [15], the bonding wires are subject to breaks and cracks due to the vibration and rotation of the car tires. Therefore, it is necessary to make some improvements in the package and electrical connection for enabling the bare MEMS chips to be mounted directly onto a printed circuit board (PCB), thereby avoiding an entire packaging level and reducing the system complexity and cost.

In this work, a novel MEMS piezoresistive pressure sensor with a self-packaged structure is presented. The sensor design and fabrication processes as well as the performance characteristics of the pressure sensor are also demonstrated.

2. Sensor design and fabrication

2.1. Sensor structure design

In our design, a pressure sensor capable of resistance to vibration and shock can be realized by using tin drag soldering instead of wire bonding to achieve the electrical connection between the electrode-pad and the external circuit, and thus the electrode-pad should have an area of at least 0.5 mm × 0.5 mm. However, for high yield in a wafer, the area of the sensor chip is usually designed to be as small as possible.

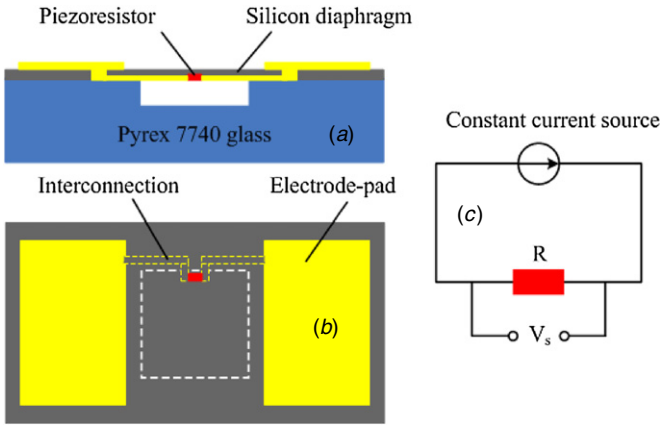

Figure 1. Schematic diagrams of (*a*) the front and (*b*) the top view of the single piezoresistive Si–glass-based pressure sensor and (*c*) the equivalent circuit.

In order to meet the design requirements, a rectangle pressure sensor, which consists of a single piezoresistive sensing (SPS) element, a Si–glass-based pressure cavity, two large-size electrode-pads and an interconnection configuration, is designed as shown in figure 1.

Figure 1 shows schematic diagrams of the front and top views of the single piezoresistive Si–glass-based pressure sensor. A Si–glass-based cavity is used to form the absolute pressure sensor. An SPS element is located on the lower surface of the silicon diaphragm and is vacuum-sealed in the Si–glass cavity (see figure 1(*a*)), which enables the piezoresistor to be physically isolated from the external environment thereby keeping it away from the influence of external harsh media. The interconnection configurations that transfer sensing signals from the SPS element to the external electrode-pads are realized by two embedded Al feedthrough lines at the bonding interface of the Si–glass to electrically connect the SPS element, and two large-area Al/Ni/Au electrode-pads are used to electrically connect with the circuit-pads in the PCB by a drag soldering technique (see figure 1(*b*)). Since Au has the advantage of high conductivity, good adhesion and general resistance to oxidation and corrosion, the Al/Ni/Au electrode-pads will provide more reliable application in harsh environments. In figure 1(*c*), a constant current source is used to power the sensor, and the applied pressure on the diaphragm, which is proportional to the output voltage V_S, can be measured by a temperature compensation method.

A special design in the sensor is that the absolute pressure cavity is formed by a self-packaged Si–glass anodic bonding process, which means that the piezo-sensing diaphragm also is a packaging protection diaphragm. The one-step Si–glass anodic bonding used in the fabrication has several advantages. Firstly, the Si–O bonds are created by the high temperature and extreme electrostatic attractive force. The Si–O bond is stronger than the Si–Si bond and is higher than the fracture strength of glass [14]; thus the vacuum sealing performance is very good for a pressure cavity. Secondly, Pyrex7740 glass has a thermal expansion coefficient nearly equal to Si at temperatures of less than 400 °C, which is helpful to minimize the thermal stress in the chip caused by the mismatch of the

thermal expansion coefficient between the glass substrate and the Si diaphragm [16]. Thirdly, the anodic bonding is less sensitive to surface imperfections (such as small particles, small steps, and low flatness and surface roughness) than Si–Si direct bonding [16]. Due to high temperature and electrostatic pressure developed during anodic bonding, the elastic, plastic or viscous deformation of the glass surface layer can overcome the surface imperfections to achieve an intimate surface contact required for bonding. Due to the fact that Si–glass bonding can give a higher yield than Si–Si bonding, the device cost will be lowered. Finally, since the glass substrate is an excellent dielectric material, it can enable the sensor to work at high temperature without any substrate leakage effect than the Si-based piezoresistive pressure sensor.

2.2. Sensor dimension design

In this design, the dimension of the sensor chip is determined according to the processing conditions and yield requirement in a wafer (no less than 4500 per wafer); thus the overall dimension of chip is designed as 1.6 mm × 1.0 mm × 0.5 μm. The design parameters include the work pressure range (P = 0–700 kPa), sensitivity (20 mV V^{-1} MPa^{-1}), resistance (R = 5000 Ω) and overload pressure ($P_{\max} = 5P$ = 3.5 MPa). Several investigations and reviews on the MEMS piezoresistive pressure sensor have described the effects of the device geometry, doping and anneal conditions on the device performance [17–21]. Referring to these studies, we can reasonably design the parameters of the pressure sensor. The thickness h and side a of a square single-crystal Si diaphragm must meet three requirements: (1) sensitivity requires the relative change in the resistance $\Delta R/R$ to be not less than 2%, (2) linearity requires the maximum deflection $g_{\max}$ in the center of the square diaphragm to be not greater than the diaphragm thickness of 20% and (3) the overload pressure $P_{\max}$ requires the difference between the longitudinal stress σ_1 and the transverse stress σ_t to be not greater than the material yield stress of 30% ($\sigma_m = 2 \times 10^9$ N m^{-2} for single-crystal Si). According to the theory of elastic deformation on plates [20], these design requirements can be expressed as follows:

$$\begin{cases} \dfrac{\Delta R}{R} = \dfrac{1}{2}\pi_{44}(\sigma_l - \sigma_t)_{\max} = \dfrac{0.308}{2}\pi_{44}P\dfrac{a^2}{h^2}(1-\nu) \geqslant 2\% \\ g_{\max} = 0.0152\dfrac{Pa^4(1-\nu^2)}{Eh^3} \leqslant 20\%\, h \\ (\sigma_l - \sigma_t)_{\max} = 0.308P_{\max}\dfrac{a^2}{h^2}(1-\nu) \leqslant 30\%\, \sigma_m \end{cases} \quad (1)$$

where π_{44} is the shear piezoresistive coefficient (π_{44} = 138 × 10^{-11} Pa^{-1}). E is Young's elastic modulus (E = 1.9 × 10^{11} N m^{-2}) and ν is the Poisson ratio ($\nu = 0.28$).

From equation (1), the range of a/h that meets the design requirements is from 19 to 27.8. According to the chip width of 1.0 mm, a reasonable side length of the Si diaphragm could be designed as 400 μm and hence the diaphragm thickness is determined as 15 μm.

In order to reduce the self-heating effect of a piezoresistor, the maximum power consumption P_c of the piezoresistor should not exceed 5 × 10^{-3} mW μm^{-2} [21]. The power consumption per unit area can be expressed as

$$P_c = \frac{I^2R_p}{WL} = \frac{I^2R_s\frac{L}{W}}{WL} = \frac{I^2R_s}{W^2}, \quad (2)$$

where I is current, R_p is the resistance of the piezoresistor, R_s is the square resistance of the piezoresistor, and W and L are the width and length of the piezoresistor, respectively. For I = 1 mA and $R_s = 250$ Ω, the width of the piezoresistor must be greater than 7 μm. Considering the processing conditions, a 10 μm width is used in the design. As a result, the length of the piezoresistor is determined as 200 μm according to the condition of $R = 5000$ Ω, which will enable the sensor to have a maximum operation current of 1.4 mA.

A 10 μm wide and 200 μm long p-type SPS element will be arranged on the edge center of a square diaphragm along the ⟨1 1 0⟩ direction in order to obtain the highest sensitivity on an n-type (1 0 0) silicon layer. The SPS element is folded into five equal sections perpendicular to the diaphragm edge, and the piezoresistive element is lightly boron-doped to about 2 × 10^{18} cm^{-3} to reduce the temperature effects on sensitivity [20].

2.3. Sensor fabrication

The Si–glass-based pressure sensors are fabricated by a standard MEMS technique. The MEMS process flow is shown in figure 2 and the main fabricating processes are given as follows.

(1) *Fabricating the piezoresistive configuration.* A standard 4-inch n-type (1 0 0) SOI wafer with a 15 μm thick Si device layer and a 0.5 μm thick buried oxide layer was used to fabricate the Si diaphragm. Firstly, the SOI wafer was oxidized, and then lithography was performed to open the SiO_2 windows by wet etching. Next, a heavily doped diffusion process was used to form the zones of the electrical connection. Thirdly, an ion-implantation process was performed to create the piezoresistive element by an Al mask. After a post-implant annealing, the resistance value is about 5000 Ω. Finally, the conductive vias were formed by depositing Al in the opened windows in heavily doped silicon (see figure 2(*a*)), and a metallization annealing process was performed to achieve good ohmic contact between Al and the heavily doped silicon.

(2) *Fabricating the cavity in Pyrex7740 wafer.* The buffered oxide etching solution was used to etch square cavities in a 4-inch 500 μm thick Pyrex7740 glass wafer. For realizing the electrical interconnection between the electrode-pads and the piezoresistive element, shallow trenches were etched in the surface of a glass wafer, and the Al feedthrough lines were created in trenches by sputtering and then a lift-off process (see figure 2(*b*)).

(3) *Fabricating the pressure sensing diaphragm.* Anodic bonding between the SOI wafer and the Pyrex7740 wafer was used to fabricate the hermetic pressure cavity, while the direct contacts between Al feedthroughs and Al vias at the bonding interface enable electrical interconnection

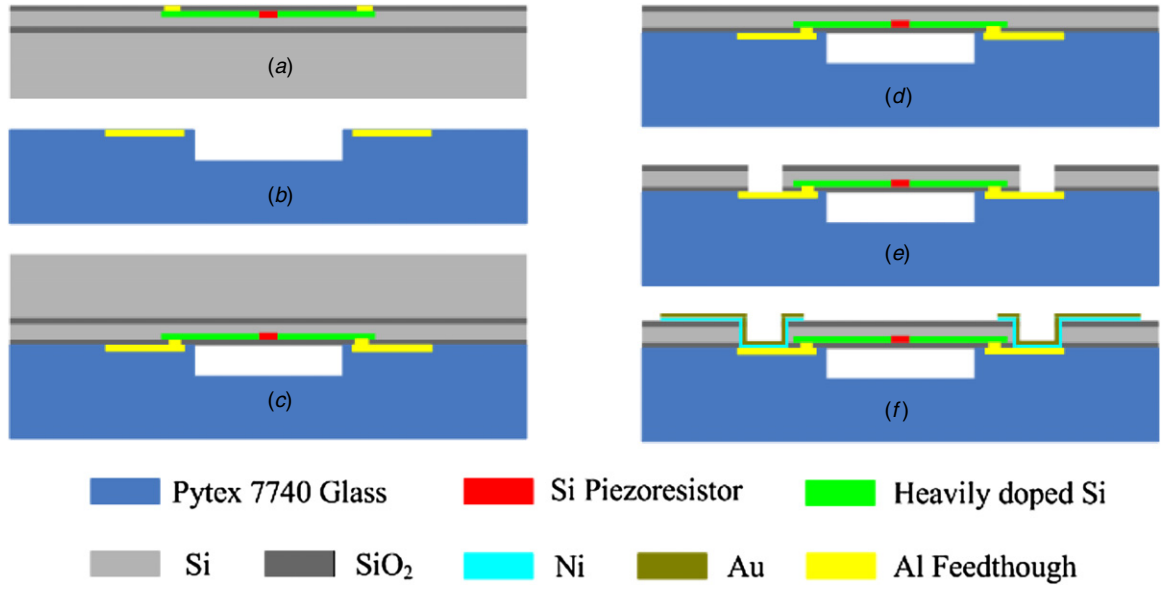

Figure 2. MEMS process flow of the Si–glass-based single piezoresistive pressure sensor.

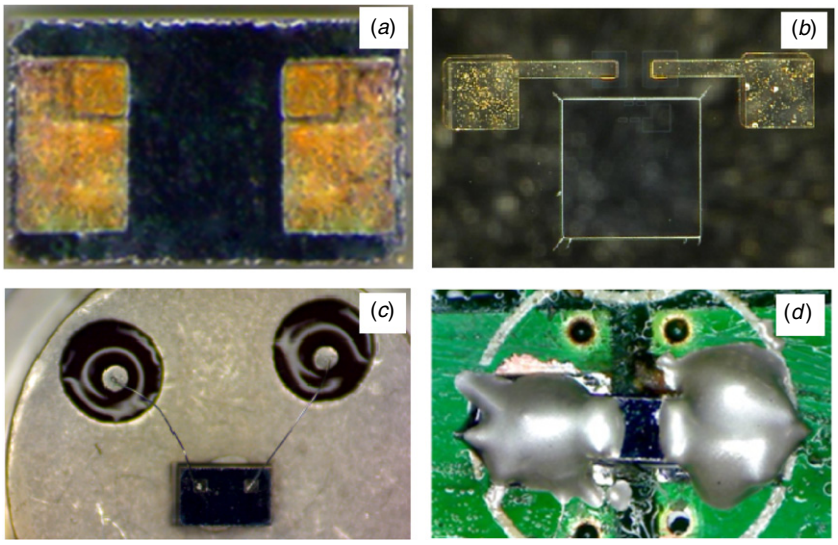

Figure 3. Micrographs before and after sensor chip packaging. (*a*) and (*b*) show the top and bottom views of the chip, respectively, and (*c*) and (*d*) show the views of sensor packaged in TO5 housing and PCB, respectively.

between the feedthroughs and the piezoresistive element (see figure 2(*c*)). After the anodic bonding, the substrate layer of SOI was removed by KOH wet etching to form the Si diaphragm (see figure 2(*d*)).

(4) *Fabricating the large-size electrode-pads*. A dry-etching process was used to open the electrode-pad windows in the Si diaphragm with the Al feedthroughs as an etch stop layer (see figure 2(*e*)). A hybrid metal Ni/Au layer was deposited in the windows and contact with the Al feedthroughs, which finally formed two large-size electrode-pads in the chip (see figure 2(*f*)).

Figure 3 shows micrographs before and after sensor chip packaging. The overall dimension of the sensor chip is 1.6 mm × 1 mm × 0.5 mm, and the dimension of the Al/Ni/Au electrode-pad is 700 μm × 450 μm (see figure 3(*a*)). The Si–glass cavity, feedthroughs and piezoresistive configuration can be seen clearly from the transparent glass substrate (see figure 3(*b*)). In figure 3(*c*), the chip was packaged in a TO5 housing with an Al wire bonding. In figure 3(*d*), the chip was mounted directly onto a PCB, and a tin drag soldering technique was used to form the interconnection between the electrode-pads and the PCB circuit.

3. Experimental results and discussion

3.1. Reliability measurements of sensors

In order to evaluate the reliability of the Si–glass self-packaging cavity, a series of tests, such as the electrical connection quality, hermetic quality and bonding strength, were suggested to certify the quality of Si–glass self-packaging structure. The test devices were designed as a 2 cm × 2 cm

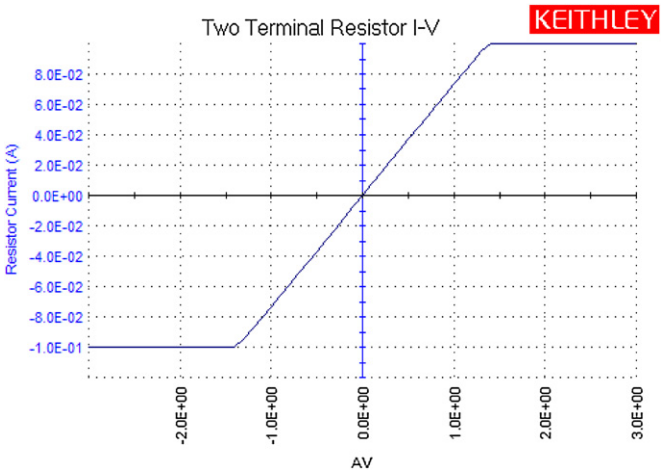

Figure 4. Electrical connection measurement between two feedthrough lines.

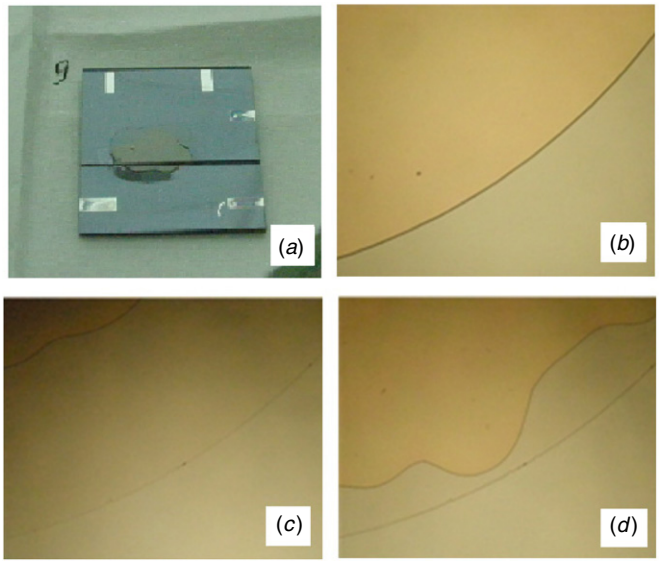

Figure 5. (*a*) Photo of the damaged device. Micrographs of IPAs testing for the (*b*) integrated device and for the damaged device after (*c*) 1 min and (*d*) 5 min.

square device with a circular hermetic cavity of 8 mm diameter. For simplifying the fabrication, the piezoresistor and large-size electrode-pads were not involved in the test devices. The embedded Al feedthrough lines were electrically connected together through the Al vias and heavily doped silicon, and the testing windows on the feedthrough lines were also opened.

A current–voltage (*I–V*) test was performed between two feedthrough lines by a Keithley CS-4200 semiconductor characterization system (see figure 4). It can be seen from figure 4 that the resistance between the feedthrough lines is about 14 Ω, which indicates that the direct contact between the Al feedthrough lines and the Al vias at the bonding interface is feasible and reliable in enabling a good electrical interconnection.

The hermeticity tests were performed in an isopropanol alcohol solution (IPAS) to certify the hermetic quality of the self-packaging cavity. Because the IPAS has better penetrability than water, it can easily penetrate into the cavity by small openings and capillary channels and thus is more suitable for leak testing. Several devices were put into the autoclave with an accelerated ageing condition of 2 atmospheric pressures, relative humidity of 100%, and 130 °C for 2 h, and then they were dipped into IPAS for three days. In order to compare the difference between the hermetic cavity and the non-hermetic cavity in IPAS testing, a device was damaged in the position of the cavity (see figure 5(*a*)) for observing the variation of the IPAS in the non-hermetic cavity. By observing through a microscope, no IPAS was observed in the hermetic cavity for all integrated devices (see figure 5(*b*)), while the IPAS penetrated into the cavity of the damaged device and gradually volatilized with time (see figures 5(*c*) and (*d*)). The tested results demonstrate that the self-packaging cavity has very good hermeticity capable of meeting the requirements for long-term sensing applications.

The bonding strength tests were performing by a tensile test setup. Both sides of the tested device were glued to the pulling rods, and then the pulling forces were applied and increased until the device was destructively pulled apart. The test results show that most of the cracking interface occurred in glass bulk, and the cracking force was about 1200 N corresponding to a bonding strength of about 3.0 MPa, which indicates that the bonding strength is very good and can meet the requirements of the hermetic package.

3.2. Performance measurements of sensors

3.2.1. Measurement theory. The piezoresistive pressure sensors commonly employ a conventional Wheatstone full bridge configuration, powered by a constant voltage source, to provide a differential voltage output proportional to the applied pressure. As the resistance change induced by temperature will be the same for all arms of the Wheatstone bridge, the temperature compensation is automatic. However, for a single piezoresistive pressure sensor, the influence of temperature cannot be avoided, which means that it is necessary to compensate for temperature by a separate on-chip temperature sensor. The temperature signals together with a pressure output signal are then digitized through an analogue-to-digital converter in a signal-processing circuit. This circuit calculates a corrected pressure signal through a pre-programmed digital correction algorithm stored in a programmable read only memory [4, 22].

When two separate sensors, a pressure sensor S_1 and a temperature sensor S_2, are used for the temperature-compensated pressure measurements, the thermal-sensing sensor S_2 must have the same configuration and physical parameters as the piezo-sensing sensor S_1 except for without a pressure cavity. When a constant current I_{cc} flows through the SPS element of the sensor S_1, the voltage drop V_{S1} across the piezoresistance can be expressed as follows:

$$V_{S1} = \left(1 - \frac{dR}{R}\right) RI_{cc} = \left(1 - \frac{dR}{R}\right) V_0, \qquad (3)$$

where V_{S1} is the output voltage of the sensor S_1, R is the resistance of the piezoresistor at pressure $P = 0$ Pa and dR/R is the relative change in piezoresistance, which depends on pressure and temperature. V_0 is the temperature dependence

of the voltage drop across the zero-stress resistance, namely $V_0 = R \times I_{cc}$. As the same current I_{cc} flows through the thermal-sensing resistor of the sensor S_2, R and V_0 can also be regarded as the resistance and output voltage of the sensor S_2, namely $V_{S2} = V_0$. Therefore, the voltage difference between the sensors S_2 and S_1 can be expressed as follows:

$$V_D = V_{S2} - V_{S1} = V_0 - \left(1 - \frac{dR}{R}\right) V_0 = \frac{dR}{R} V_0. \quad (4)$$

When the doping concentration is constant, in terms of the applied pressure P and input current I_{cc}, the output V_D can also be expressed as

$$V_D = \frac{dR}{R} V_0 = Pc\pi R I_{cc}, \quad (5)$$

and

$$\pi R = \pi_0(1 + TC\pi \cdot \Delta T)R_0(1 + TCR \cdot \Delta T), \approx \pi_0 R_0[1 + (TC\pi + TCR)\Delta T] \quad (6)$$

where c is a constant related to the diaphragm structure of the pressure sensor S_1. The piezoresistive coefficient π is a function of temperature. π_0 and R_0 are the piezoresistive coefficient and resistance at the condition of zero temperature and zero pressure, respectively. $TC\pi$ and TCR are the temperature coefficients of π and resistance, respectively. ΔT is the temperature variation. According to equations (5) and (6), the temperature coefficient of sensitivity (TCS) of the pressure sensor is decided by

$$TCS = TC\pi + TCR. \quad (7)$$

Generally, $TC\pi$ is negative and TCR is positive, and both $TC\pi$ and TCR depend on doping concentration. It has been proved experimentally that $TC\pi$ and TCR have the same value (but with opposite signs) at two critical doping levels: $N \cong 2 \times 10^{18}$ cm^{-3} and $N \cong 5 \times 10^{20}$ cm^{-3} [20]. Therefore, if the doping level of the resistor is controlled to be equal to one of the two critical doping levels, the TCS of the pressure sensor will be zero due to the cancellation of $TC\pi$ and TCR. As a result, the pressure P applied to the pressure sensor will be proportional to the voltage difference between the pressure sensor S_1 and the temperature sensor S_2 (see equations (5) and (6))

3.2.2. Measurement results and discussion. The output characteristics of the pressure sensors were measured by a pressure test system that consists of a pressure chamber with a heater, a pneumatic tester, a gas source and an electronic control and measurement system. Figure 6 shows the schematic diagram of the pressure test system. The pneumatic tester (GE P3000) is a high precision pressure test and control system. A constant current of 1 mA provided by a dc power supply (Agilent E3612A) was applied to the input of the pressure sensor. At each applied pressure, the sensor output was measured by a digital multimeter (Agilent 34401A). The test temperatures were controlled by a PID digital temperature controller.

Experimentally, the pressure varied from 0 to 700 kPa, and the output voltage was recorded regularly every 50 kPa under different temperature conditions. In the practical

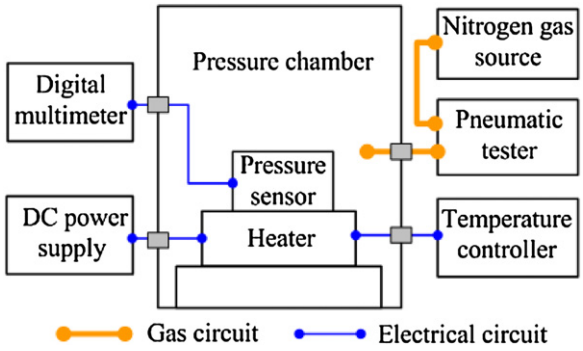

Figure 6. Schematic diagram of the pressure test system.

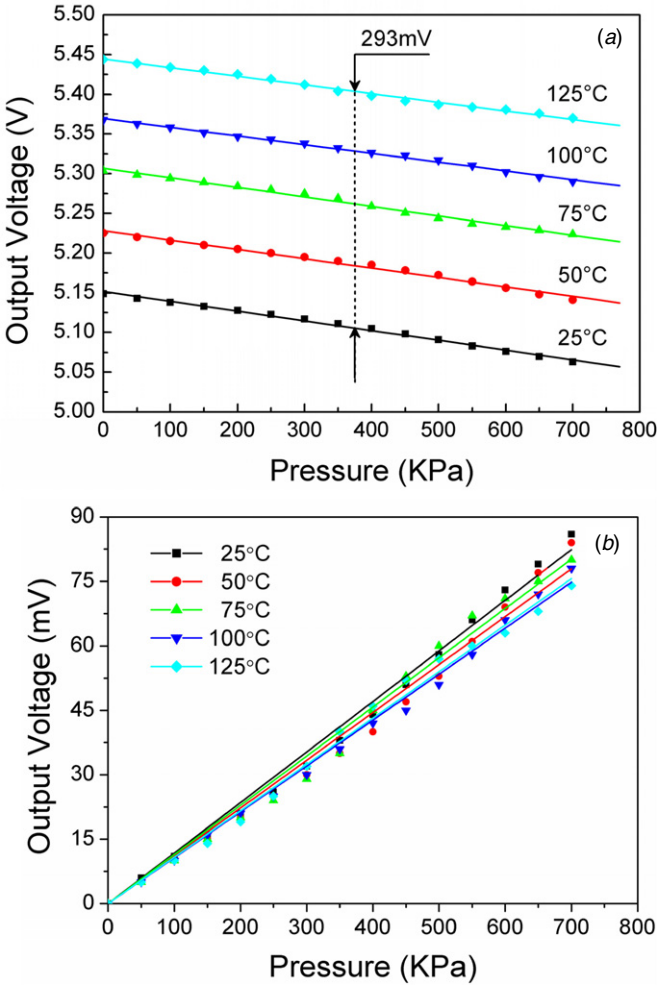

Figure 7. *V–P* characteristics of the pressure sensor at different temperature conditions (*a*) before and (*b*) after the temperature compensations.

pressure and temperature measurements, only one pressure sensor was used in this experiment. The temperature sensing signal was obtained by a voltage–temperature measurement for the pressure sensor at zero-pressure condition. By using equation (2), the difference between the output voltage at zero pressure and the output at operating pressure is proportional to the applied pressure.

Figure 7 shows the voltage–pressure (*V–P*) characteristics of the single piezoresistive pressure sensor at different

Table 1. Main performance characteristics of the single piezoresistive pressure sensor.

Parameters		Unit	Typical value
Full scale	25 °C	kPa	700
Supply current	25 °C	mA	1.0
Full scale output	25 °C	mV	86
Offset	(25–125 °C)	mV	0
Sensitivity	25 °C	mV V^{-1} MPa^{-1}	24
Nonlinearity	(25–125 °C)	% FS	⩽5.2
Temperature coefficient of offset (TCO)	(25–125 °C)	% FS $°C^{-1}$	0 0
Temperature coefficient of sensitivity (TCS)	(25–125 °C)	% FS $°C^{-1}$	0.14

temperature conditions before and after temperature compensation. It can be found from figure 6(*a*) that the linearity of *V–P* curves is very good, but the resistance changes due to temperature enable a voltage drift of about 293 mV when the temperatures vary from 25 to 125 °C. After performing the temperature compensations by voltage differences, the *V–P* curves show the typical output characteristics of a Wheatstone full bridge pressure sensor operated with a constant voltage of 5 V. By least-squares fitting for measurement data, the main performance characteristics can be obtained and listed in table 1.

In comparison with Wheatstone full bridge pressure sensors, the single piezoresistive pressure sensors have four distinguishing features. Firstly, the sensitivity of the pressure sensors reaches 24 mV V^{-1} MPa^{-1}, which is comparable to that of Wheatstone full bridge pressure sensors. It means that the pressure sensors can provide the same voltage output as that of Wheatstone full bridge pressure sensors, but achieve such with a single piezoresistive element rather than 4. Secondly, the pressure sensors have low TCS (about 0.14% FS $°C^{-1}$), by contrast, the TCS of Wheatstone full bridge sensors are generally no less than 0.2% FS $°C^{-1}$ when constant voltage supply is used. This can be attributed to the compensation for TCS in an appropriate doping concentration by the use of constant current supply instead of the use of constant voltage supply. Thirdly, since the temperature compensation for the pressure sensor is based on the temperature dependence of the voltage output at zero pressure, both the zero-point offset and the temperature coefficient of offset (TCO) are both equal to zero. Finally, the nonlinearity of the pressure sensors is 5.2% FS, which is far larger than that of the Wheatstone full bridge sensors, which will worsen the accuracy of the pressure sensor considerably. The reason for such a large nonlinearity may be due to the balloon effect proposed by Bhat [23]. In Bhat's article, the nonlinearity is affected by both the stretching stress and bending stress in the diaphragm. The nonlinearity caused by the balloon effect is smaller when the sensor is subjected to pressure applied from the front side where the piezoresistor is located, whereas the nonlinearity is larger when the pressure is applied from the backside as is the case shown in figure 1. The balloon effect can be avoided by the optimal design of the diaphragm geometry, for example, the use of a bossed diaphragm [24].

4. Conclusion

A Si–glass-based single piezoresistive pressure sensor was designed and fabricated by a standard MEMS technique for harsh environment applications. The pressure sensors have three highlights in structure design. (1) The pressure sensor is designed as a self-packaged Si–glass structure, which enables the piezo-sensing element to be on the lower surface of the silicon diaphragm and vacuum-sealed in the Si–glass cavity. (2) The piezo-sensing configuration of the pressure sensor is designed as an SPS element, which is electrically connected to the electrode-pads by the embedded Al feedthrough lines at the bonding interface of Si–glass through the Al vias and the heavily doped diffusion zones. (3) Two larger size electrode-pads are designed for realizing the soldered electrical connection between the sensor and the external circuit. The performance of the pressure sensors was characterized by pressure measurement from 0 to 700 kPa at temperatures ranging from 25 to 125 °C. The temperature compensation was performed by the difference between the output voltage at zero pressure and the output at operating pressure. The measured results show the sensitivity and the temperature coefficient of sensitivity reach 24 mV V^{-1} MPa^{-1} and 0.14% FS $°C^{-1}$, respectively, and both the zero-point offset and TCO are equal to zero, which are able to meet the commercial application requirements. However, a nonlinearity of 5.2% FS caused by the balloon effect will considerably worsen the accuracy of the pressure sensors. It is suggested to reduce the balloon effect by using a bossed diaphragm in the pressure sensor.

Acknowledgments

This work was supported in part by the National Natural Science Foundation of China (nos 51075344, 61274120 and 51175444), in part by Fujian Province Major Projects on University–Industry Cooperation in Science and Technology (no 2013H6023), and in part by Science and Technology Program of Xiamen (nos 3502Z20123008 and 3502Z20126006).

References

[1] Barlian A A, Park W T, Mallon J R, Ali J, Rastegar J and Pruitt B L 2009 Review: semiconductor piezoresistance for microsystems *Proc. IEEE* **97** 513–52
[2] Pramanik C, Saha H and Gangopadhyay U 2006 Design optimization of a high performance silicon MEMS piezoresistive pressure sensor for biomedical applications *J. Micromech. Microeng.* **16** 2060–6
[3] Giulio F, Lasse L and Erik V T 2010 Novel designs for application specific MEMS pressure sensors *Sensors* **10** 9541–63
[4] Guo S W, Eriksen H, Childress K, Fink A and Hoffman M 2009 High temperature smart-cut SOI pressure sensor *Sensors Actuators* A **154** 255–60
[5] Pakula L S, Yang H, Pham H T M, French P J and Sarro P M 2004 Fabrication of a CMOS compatible pressure sensor for harsh environments *J. Micromech. Microeng.* **14** 1478–83
[6] Aravamudhan S and Bhansali S 2007 Reinforced piezoresistive pressure sensor for ocean depth measurements *Sensors Actuators* A **142** 111–7

[7] Fraga M A, Furlan H, Oliveira I C and Rasia L A 2011 Preliminary evaluation of the influence of the temperature on the performance of a piezoresistive pressure sensor based on a-SiC film *Microsyst. Technol.* **17** 477–80
[8] Zhang H X, Guo H, Wang Y, Zhang G B and Li Z H 2007 Study on a PECVD SiC-coated pressure sensor *J. Micromech. Microeng.* **17** 426–31
[9] Li X, Pang S X, Xu K X and Tang H 2012 High-temperature piezoresistive pressure sensor based on implantation of oxygen into silicon wafer *Sensors Actuators* A **179** 277–82
[10] Zhao Y L, Jiang Z D and Zhao L B 2010 An ultra-high pressure sensor based on SOI piezoresistive material *J. Mech. Sci. Technol.* **24** 1655–60
[11] Chou T, Chu C, Lin C and Chiang K 2009 Sensitivity analysis of packaging effect of silicon-based piezoresistive pressure sensor *Sensors Actuators* A **152** 29–38
[12] Krassow H, Campabadal F and Lora-Tamayo E 1999 Wafer level packaging of silicon pressure sensors *Sensors and Actuators* A **82** 229–33
[13] Lee B, Seok S and Chun K 2003 A study on wafer level vacuum packaging for MEMS devices *J. Micromech. Microeng.* **13** 663–9
[14] Najafi K 2003 Micropackaging technologies for integrated microsystems: applications to MEMS and MOEMS *Proc. SPIE* **4979** 1–19
[15] Wei C Z, Wang Q, Xia X Y and Li X X 2012 TPMS (tire-pressure monitoring system) sensors: monolithic integration of surface-micromachined piezoresistive pressure sensor and self-testable accelerometer *Microelectron. Eng.* **91** 167–73
[16] Lindroos V, Tilli M, Lehto A and Motooka T 2010 *Handbook of Silicon Based MEMS Materials and Technologies* (Oxford: Elsevier)
[17] Bae B, Flachsbart B R, Park K and Shannon M A 2004 Design optimization of a piezoresistive pressure sensor considering the output signal-to-noise ratio *J. Micromech. Microeng.* **14** 1597–607
[18] Kanda Y 1997 Optimum design considerations for silicon piezoresistive pressure *Sensors Actuators* A **62** 539–42
[19] Merlos A, Santander J, Alvarez M D and Campabadal F 2000 Optimized technology for the fabrication of piezoresistive pressure sensors *J. Micromech. Microeng.* **10** 204–8
[20] Bao M H 2005 *Analysis and Design Principles of MEMS Devices* 1st edn (Amsterdam: Elsevier)
[21] Sun Y C, Liu Y L and Meng Q H 2000 *Pressure Sensor: Design, Manufacture and Application* (Beijing: Metallurgical Industry Press)
[22] Yang C 2011 The compensation for hysteresis of silicon piezoresistive pressure sensor *IEEE Sens. J.* **11** 2016–21
[23] Bhat K N 2007 Reviews: silicon micromachined pressure sensors *J. Indian Inst. Sci.* **87** 115–31
[24] Sandmaier H and Kuhl K 1993 A square-diaphragm piezoresistive pressure sensor with a rectangular central boss for low-pressure ranges *IEEE Trans. Electron Devices* **40** 1754–9